EARTHQUAKE ENGINEERING AND STRUCTURAL DYNAMICS, VOL. 26, 251–268 (1997)

RESPONSE SPECTRA FOR DIFFERENTIAL MOTION OF COLUMNS

MIHAILO D. TRIFUNAC AND MARIA I. TODOROVSKA

University of Southern California, Department of Civil Engineering, Los Angeles, CA 90089-2531, U.S.A.

SUMMARY

The validity of the response spectrum concept for determining loads in structures excited by differential earthquake ground motion is examined. It is shown that the common definition of response spectrum for synchronous ground motion can be reconciled to remain valid in cases when the columns of extended structures experience different motions. Then, a relative displacement response spectrum for design of first-storey columns, $\mathrm{SDC}(T, \delta, \zeta, \tau)$, is defined. In addition to natural period, T, and fraction of critical damping, ζ, this spectrum depends also on the 'travel time', τ (of the waves in the soil over distances about one half width, or length of the structure), and on a factor, δ, specifying the relative displacement of the first floor. It is shown how this spectrum can be determined using existing empirical scaling equations for relative displacement spectra $\mathrm{SD}(T, \zeta)$ and for peak velocity and peak acceleration of strong ground motion. These new spectra are illustrated for a horizontal component of a record in the near field of the 1994 Northridge earthquake. The results show that differential motions are more important for short period (stiff) than for longer period (flexible) structures, and for structures founded on softer ground (small shear wave velocity).

KEY WORDS: differential motions; multiple support excitation; response spectrum

INTRODUCTION

The response spectrum functional was introduced in 1930s,[1,2] but, because of the lack of representative strong motion recordings, it took 30 years (until the end of 1960s and early 1970s) for it to became the common scaling tool in the analysis of earthquake resistant structures.[3] Since the 1960s, the response spectrum amplitudes have been scaled in terms of absolute peak ground acceleration.[4] In the mid-1970s, direct scaling of spectral amplitudes was introduced.[5–7] Response spectrum superposition, for analysis of multi-degree-of-freedom (MDOF) systems, has evolved from the first idea of using the sum of absolute maxima of modal responses[8] to detailed methods using probability density functions of peak amplitudes of relative response.[9] Today, this method considers explicitly the effects of modal interaction, soil–structure interaction and other statistical properties of the peaks of relative response.[10–17]

For many design analyses, the earthquake shaking can be specified at a single point, and the spatial variation of motion at multiple supports of structures may be neglected. When the distances between the multiple support points are large (bridges, dams, tunnels, long buildings), the effects of differential motions become important and should be considered in dynamic analyses.[18] Spatial and temporal characteristics of strong earthquake motion required for such analyses have been investigated recently.[19–21] The consequences of differential ground motion have been studied for the response of beams,[22–24] bridges.[25–27] simple models of three-dimensional structures,[28] long buildings[29–32] and dams.[33–35] However, with few exceptions, engineering applications of the response spectrum method ignore the wave propagation effects in the foundation soil, or consider only stochastic representation of the differences in motion among separate supports.[36–38]

Okubo *et al.*[39] were among the first to measure and interpret finite ground strains of recorded earthquake motions, for plan dimensions representative of intermediate and large buildings. They showed that, for short-period (stiff) structures, finite ground strains will lead to increased base shears. Zembaty and

CCC 0098–8847/97/020251–18

Received 21 February 1996
Revised 10 September 1996

Krenk[40,41] studied the same model via random vibration based shear force response spectrum, addressing explicitly the contribution of quasi static and dynamic terms in the response. They showed that although the relative response of the structure is reduced in case of differential motion of the supports (due to 'averaging' of spatially correlated motions), the shear force in the columns, which for stiff structures primarily depends on the quasi-static contribution to the response, may be significantly larger than for synchronous excitation. Their qualitative description of the problem leads to the same conclusions as the direct approach in this paper, but requires 'calibration' before it can be applied to engineering calculations.

The purpose of this paper is to show how the elementary form of the response spectrum method can be reconciled with and extended to include effects of differential motion of structures on multiple supports. Without any loss of generality, the model used considers only horizontal ground motion. Only models of a one storey structure and a simple, first-mode approximation of response of a multi-storey structure are considered. Tall structures, modelled by an n degree-of-freedom system, are briefly discussed, but detailed analysis is beyond the scope of this paper. Analyses of amplitudes of the ordered peaks of response, interaction of different modes, and of soil–structure interaction,[10–17] as those influence shear forces in the first-storey columns, will be examined in future studies.

THE MODEL

Assumptions

The nature of relative motion of individual column foundations or of the entire foundation system will depend on the type of foundation and stiffness of the connecting beams and slabs, the characteristics of the soil surrounding the foundation, the type of incident waves, and on the direction of wave arrival. In reality, at the base of each column, the motion has six degrees of freedom. Figure 1 illustrates schematically an example of column deformations in the first storey of a 'building', during passage of Rayleigh waves, propagating along its longitudinal axis. During actual strong motion, the direction of wave arrival is arbitrary, the structure is excited simultaneously by different types of waves, leading to more complex and three-dimensional deformation of the columns. This will also cause warping of the ground surface and of the building foundation, and will increase the twisting deformation of the columns . From Figure 1 it is seen that, even in case of Rayleigh waves only, the body of this structure is also deformed by the passage of seismic waves.[32] This would require more than one degree of freedom in the response analysis, which is beyond the scope of this paper.

For simplicity, we consider only the horizontal component of relative motion of column foundations. Laterally homogeneous (parallel layers) earth model is assumed, deforming elastically. Without loss of generality, we assume that the longitudinal axis of the structure (x-axis) coincides with the radial direction

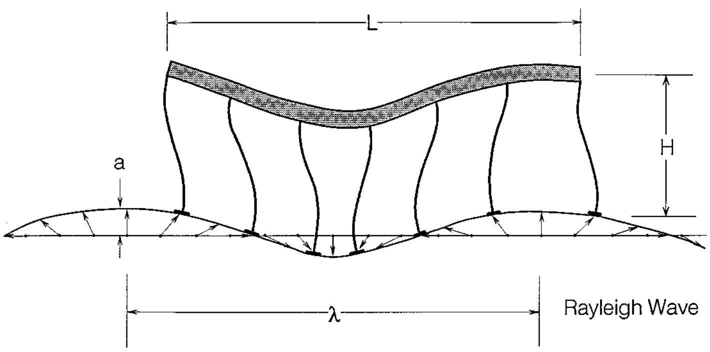

Figure 1. A structure excited by passage of a Rayleigh wave

(r-axis) of the propagation of waves from the earthquake source. It is also assumed that the structure is far away from the earthquake source, so that the ground motion can be represented as a superposition of plane (body and surface) waves, of the form

$$f(z)\mathrm{e}^{\mathrm{i}\omega(t - x/c_x(\omega))},$$

where $f(z)$ is some function of depth,[29–35] and $c_x(\omega)$ is the velocity with which the phase propagates in the x-direction. For body (P and S) waves, c_x will depend on the incident angle, and for surface waves-on the dispersion characteristics of the medium ($c_x(\omega)$ will be different for each of the surface wave modes). For parallel layers with shear wave velocity increasing with depth, $c_x(\omega)$ of the surface waves is greater than the velocity of the top ('slowest') layer, and smaller than the velocity in the bottom ('fastest') layer. For this model, the rotational components of motion will reduce to rotation about the vertical axis, z, representing 'torsional' excitation caused by passage of SH and Love waves,[42] and to 'rocking' about the y axis.[43] If the structure is oriented arbitrarily, e.g. the x-axis and the r-axis are at an angle φ, then $c_x(\omega) = c_r(\omega)/\cos\varphi$, where $c_r(\omega)$ is the phase velocity in the radial direction, determined by dispersion analysis.

The complexity of the analysis would be reduced if some equivalent, constant in time, phase velocity c_{eq} could be used, representative for all the surface wave modes and all the body waves of the ground motion propagating between the supports of the structure. Further, it would be convenient to relate c_{eq} to the average shear wave velocity of waves in the top 30 m below the surface,[44,45] β_{av}, which can be determined by measurement. The 'proportionality function' relating the two velocities, e.g. the function A in $c_{\mathrm{eq}} \approx \beta_{\mathrm{av}}/A$, can be determined on the basis of region-specific empirical studies or by site-specific numerical simulations. Numerical simulations of artificially generated ground motion in parallel layers[44] suggest that, for a typical range of magnitudes and epicentral distances, the function A is of the order of unity. For body waves, c_{eq} will depend on β_{av} and on the incident angle ($c_{\mathrm{eq}} \sim \beta_1/\sin\gamma$, where γ is the angle between the incident ray and the vertical), and c_{eq} can be large relative to β_{av} for nearly vertical incidence. For soft surface soil and sediments $\gamma \to 0$, and thus it may not be unusual to find c_{eq} in the range between 1 and 6 km/s[46,47] for incident body waves. The contribution of surface waves will dominate at larger epicentral distances and for faulting through soft surface sediments, typical of many Southern California earthquakes.[48] For shallow and surface faulting, most of the strong motion energy will be associated with surface waves.[48] Ongoing studies of recorded differential motions in Pasadena, during Whittier-Narrows earthquake of 1987 and for the Hollister differential array[49] (these include all types of waves) show that the average value of A may decrease from ~ 1.7, at zero separation distances, towards 0.4, for ~ 150 m separation. In this paper, we will assume that $c_{\mathrm{eq}} \approx \beta_{\mathrm{av}}$, i.e. $A = 1$.

In this paper, analysis will be performed for structures on isolated foundations only. When the design conditions or local codes require connecting beams or slabs, depending on the relative rigidity and on the strength of these connecting members, differential motions in the first-storey columns will be reduced or eliminated. In those cases, the components of the interconnected foundations will be designed to withstand the forces caused by the differential motions and by strains in the soil during passage of seismic waves. We first analyse a one-storey structure supported by multiple columns, and derive response spectra that account for differential motions of the supports. Then, we suggest how the results can be generalized to multi-storey buildings.

Equation of motion for a one-storey structure with asynchronous base excitation

We first consider the model shown in Figure 2. It is a one-storey structure with mass m supported by n columns with stiffness k_i, $i = 1, \ldots, n$. Let $u_i(t)$ be the absolute displacement of the base of column i. Displacements $u_i(t)$ are in general all different, as a result of the wave passage. Let u_G be the absolute displacement of the mass. The absolute displacement of the top of all columns is also u_G, as we assume the slab supporting the mass of the structure to be rigid.

We now write an equation of motion for this structure of form similar to the familiar form for a SDOF oscillator subjected to synchronous base motion, with the help of a point R (on the ground) which we will use as reference. We denote the absolute displacement of point R by $u_0(t)$, and we assume that it can be specified.

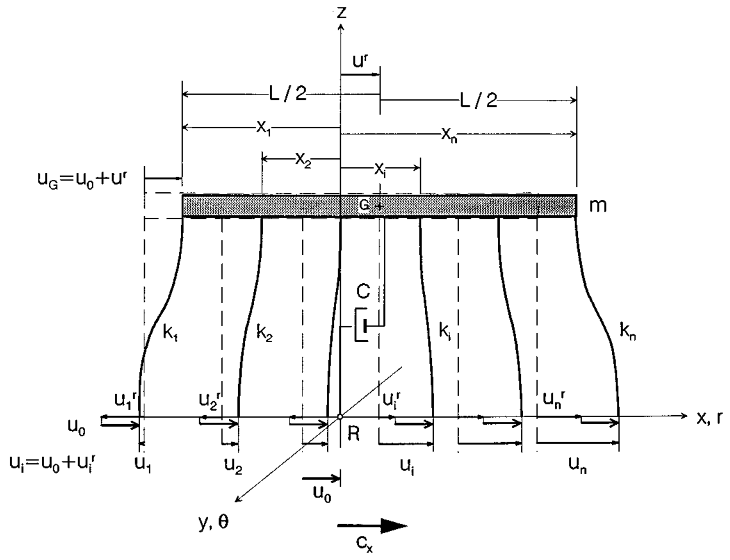

Figure 2. A model of a one-storey structure excited by general differential ground motion in the horizontal direction only. The columns have stiffness k_i, $i = 1, \ldots, n$, and the mass of the structure is m. The absolute displacement of the base of the columns is u_i. Point R and the z-axis move with displacement u_0 that satisfies the condition $\sum_1^n k_i u_i = u_0 \sum_1^n k_i$. The displacement of the mass relative to point R is u^{r}

We assume that the damper (with damping coefficient C) is connected between the rigid slab and this point R. Next, we express the absolute displacements of the mass and of the base of the columns as a sum of $u_0(t)$ and the respective relative displacements, $u^{\mathrm{r}}(t)$ and $u_i^{\mathrm{r}}(t)$,

$$u_G(t) = u_0(t) + u^{\mathrm{r}}(t) \tag{1}$$

and

$$u_i(t) = u_0(t) + u_i^{\mathrm{r}}(t) \tag{2}$$

Dynamic equilibrium of the mass implies

$$m(\ddot{u}_0 + \ddot{u}^{\mathrm{r}}) + C\dot{u}^{\mathrm{r}} + \sum_{i=1}^{n} k_i[(u_0 + u^{\mathrm{r}}) - (u_i)] = 0 \tag{3}$$

If we can choose point R so that its displacement $u_0(t)$ satisfies the condition

$$\sum_{i=1}^{n} k_i(u_0 - u_i) = 0 \tag{4}$$

or

$$u_0 = \frac{\sum_{i=1}^{n} k_i u_i}{\sum_{i=1}^{n} k_i} \tag{5}$$

then, after substituting this condition into equation (3), it follows that

$$m\ddot{u}^{\mathrm{r}} + C\dot{u}^{\mathrm{r}} + u^{\mathrm{r}} \sum_{i=1}^{n} k_i = -m\ddot{u}_0 \tag{6}$$

Further, introducing circular frequency ω and damping ratio ζ such that

$$\omega^2 = \sum_{i=1}^{n} k_i/m \tag{7}$$

and

$$2\omega\zeta = C/m \tag{8}$$

equation (6) becomes

$$\ddot{u}^{\mathrm{r}} + 2\omega\zeta\dot{u}^{\mathrm{r}} + \omega^2 u^{\mathrm{r}} = -\ddot{u}_0 \tag{9}$$

Equation (9) is the classical equation of motion of a SDOF oscillator, with natural frequency ω and damping ratio ζ, excited by synchronous acceleration of the base $\ddot{u}_0$, and u^{r} is the displacement relative to the base. By the definition of response spectrum, the peak of the relative response, $|u^{\mathrm{r}}_{\max}|$, is the spectral displacement $\mathrm{SD}(T, \zeta)$ for the motion u_0 ($T = 2\pi/\omega$ is the natural period of the oscillator). The above demonstrates that response spectrum of ground motion for a carefully chosen reference point (R) can be used to determine the peak relative response amplitude (relative with respect to that reference point).

It is seen from equation (5) that the displacement of the reference point, u_0, is a weighted average of the absolute displacements at the base of the individual columns, u_i, the weighting factors being proportional to the stiffness of the columns. If the displacements u_i are arbitrary, then the location of point R (with respect to undeformed configuration) changes with time. However, motions at the base of columns of a structure during an earthquake are not completely arbitrary and can be related to each other, via the strain field in the ground.[44,45] The following section presents an approximate representation of the excitation of individual columns, u_i, that can lead to response spectra for design of columns of first storey of a long structure.

Ground motion representation for asynchronous column excitation

Let x_i be the distance from the ith column to point R in the undeformed configuration (Figure 2). When this distance is small compared to the dominant wavelengths of ground motion ($|x_1|, \ldots, |x_n| \ll (2\pi/\omega)c_x$), we approximate the displacement at the base of the ith column by a second-order Taylor series expansion of u_i about u_0

$$u_i(t) \approx u_0(t) + \left.\frac{\partial u}{\partial x}\right|_{x = x_R} x_i + \frac{1}{2}\left.\frac{\partial^2 u}{\partial x^2}\right|_{x = x_R} x_i^2 \tag{10}$$

Then, the relative motion of the base of the ith column, u_i^{r}, is

$$u_i^{\mathrm{r}}(t) \approx \left.\frac{\partial u}{\partial x}\right|_{x = x_R} x_i + \frac{1}{2}\left.\frac{\partial^2 u}{\partial x^2}\right|_{x = x_R} x_i^2 \tag{11}$$

When the horizontal wave propagation in the soil is ignored or is not present (for example, for vertically incident plane waves, c_x is infinite), all $u_i^{\mathrm{r}} \equiv 0$, and points on the ground surface move as u_0. Thus, u_i^{r}, $i = 1, \ldots, n$, represent local relative motions in the soil caused by wave passage.

We recall that $\partial u/\partial x = \varepsilon_{xx}$, and so the first term in Equation (11) is proportional to the strain in the soil. For a site on parallel layers, in the absence of complex three-dimensional interference and scattering, this strain component ε_{xx} can be approximated by

$$\varepsilon_{xx}(t) = \frac{\partial u(t)}{\partial x} \approx -A\frac{v(t)}{\beta_{\mathrm{av}}} \tag{12}$$

and β_{av} is the average shear wave velocity in the top 30 m of soil, $v(t)$ is the particle velocity, and A is an empirical scaling function which can be estimated from numerical simulations of strong motion at a given site[44] (recall the discussion on equivalent phase velocity $c_{\mathrm{eq}} \approx \beta_{\mathrm{av}}/A$ in the section on the assumptions in this analysis). Therefore, $(\partial u/\partial x)x_i$ in equations (10) and (11) can be approximated by

$$\frac{\partial u}{\partial x}x_i \approx -A\frac{v(t)}{\beta_{\mathrm{av}}}x_i = -v(t)\tau_i \tag{13}$$

where

$$\tau_i = A x_i/\beta_{av} \tag{14}$$

is the time (modified by function A) it takes a wave propagating horizontally with velocity β_{av} to go from point R (see Figure 2) to the base of the ith column. Using the same type of approximate analysis, we write

$$\frac{1}{2}\frac{\partial^2 u}{\partial x^2}(x_i)^2 \approx \frac{1}{2}a(t)\tau_i^2 \tag{15}$$

where $a(t) = \partial^2 u/\partial t^2$ is the acceleration of the ground at point R. Then

$$u_i^r(t) \approx -v(t)\tau_i + \tfrac{1}{2}a(t)\tau_i^2 \tag{16}$$

For the approximations in equations (13) and (15) to be meaningful, it is necessary that $x_i \ll L_p/4$, where L_p is the prevalent wavelength present in ground motion. By 'prevalent' we mean the wavelength which is near the peak of the corresponding Fourier amplitude spectrum of ground motion. We represent L_p by $T_p c$, where T_p is the period of that motion and c is the corresponding phase velocity. T_p is in the range[5] from about 0·5 s (for $M = 4{\cdot}5$) to about 1·0 s (for $M \sim 7{\cdot}5$), and so the approximate range for the smallest L_p becomes $0{\cdot}5\,\beta_{av} < L_p < 1{\cdot}0\,\beta_{av}$ (since $c \geqslant \beta_{av}$). Because $-v(t)\tau_i + \tfrac{1}{2}a(t)\tau_i^2$ is a parabola in τ_i, equation (16) would have no meaning unless x_i is smaller than one quarter of the prevailing wave length, $x_i < L_p/4$. This suggests $\tau_{max} \approx A0{\cdot}5\,\beta_{av}/4\beta_{av} \approx 0{\cdot}10$ s (assuming[44] $A \sim 0{\cdot}4$ to 1). The Fourier amplitude spectrum of $v(t)$ is equal to $1/\omega$ times the Fourier amplitude spectrum of $a(t)$ and therefore T_p for velocity spectra (i.e. for $v(t)\tau_i$) would be longer than the T_p for acceleration spectra. Thus, the above approximate reasoning would allow larger τ_{max} based on velocity of motion than $\tau_{max} \sim 0{\cdot}10$ s that we estimated for the acceleration.

Horizontal 'dimensions' of structures and typical values of x_i will depend on site and response factors and cannot be grouped easily into one or two parameter representations. For example, many modern tall buildings have plan dimensions in the range[50] from about 20 to 80 m and so, for such buildings, the largest x_i would be of the order of 40 m. For continuous multi-span bridges, x_i can be larger. In the Los Angeles area, the smallest shear wave velocity in the soil in the top 30 m is typically about 300 m/s, while the largest, for sites on basement rock, may approach ~ 1000 and occasionally 2000 m/s. Thus it is useful to have results for the range of τ between, $\tau_{max} \approx 40/300 = 0{\cdot}13$ and $\tau_{min} \approx 10/2000 = 0{\cdot}005$. Based on these estimates (and on the above limits on τ such that $x_i < L_p/4$), we will consider $0{\cdot}001 < \tau_i < 0{\cdot}1$.

The number and the orientation of the existing strong motion instruments in buildings and the data recorded so far are not adequate to evaluate independently the accuracy of the above approximation (equation (16)) and for how large τ_i it may approximate the differential motions. Thus it is useful to deploy strong motion instruments in and near foundations of structures, to gather such data from future earthquakes. The validity of equation (16) can also be tested by numerical modelling using the computer program SYNACC[42,43,51,52] for simple representation of site geology, by a set of parallel layers.[44]

Location of reference point R

For a constant strain field, ε_{xx}, in the ground between the columns, equation (9) can be associated with reference point R fixed to a point on the ground surface (and moving as $u_0(t)$) at $\eta = \ell_R$, where η is measured from the point in the centre of the horizontal projection of the rigid mass m (Figure 2), and

$$\ell_R = \sum_{i=1}^{n} k_i \eta_i \Big/ \sum_{i=1}^{n} k_i \tag{17}$$

For intermediate and small τ_i (e.g. $\tau_i < 0{\cdot}01$) the term $\tfrac{1}{2}a(t)\tau_i^2$ in equation (16) may be neglected. The approximation $u_i^r(t) \approx -v(t)\tau_i$ then corresponds to the constant strain approximation.

For some general but deterministic, as well as for the nondeterministic (stochastic) representations of u_i, $u_0(t)$ can always be defined in terms of equation (5), and the relative response $u^r(t)$ can be computed from equation (9) relative to $u_0(t)$, but the position of the reference point R will in general be a function of time. For practical computation of shear forces in the columns, it may be useful to define a position of R from the mean

value of $u_0(t)$ taken over the entire period of excitation (by measuring all x_i's from that point, the τ_i's, now functions of time, can be approximated by their constant mean amplitudes, as long as the motion of R is small relative to x_1 and x_n). Analysis of such cases suggests that the effects associated with variations of the position of reference point R are usually small and may be neglected, but are beyond the scope and the expected use of the simplified model shown in Figure 2.

Response spectra for differential motion of columns of a one-storey structure

The shear forces, V_i, $i = 1, \ldots, n$, in the columns of the one-storey structure in Figure 2 are equal to

$$V_i(t) = k_i[u_0(t) + u^{\mathrm{r}}(t) - u_i(t)] \tag{18}$$

After the substitution for $u_i(t)$ from equation (2),

$$V_i(t) = k_i[u^{\mathrm{r}}(t) - u_i^{\mathrm{r}}(t)] \tag{19}$$

and after approximating $u_i^{\mathrm{r}}(t)$ by the expression in equation (16)

$$V_i(t) = k_i[u^{\mathrm{r}}(t) + v(t)\tau_i - \tfrac{1}{2}a(t)\tau_i^2] \tag{20}$$

where $v(t)$ and $a(t)$ are the ground velocity and the ground acceleration for reference point R, $v(t) = \partial u_0(t)/\partial t$ and $a(t) = \partial^2 u_0(t)/\partial t^2$.

To design the columns for maximum shear, the maximum relative displacement $u_i^{\mathrm{r}}(t) = -v(t)\tau_i + \frac{1}{2}a(t)\tau_i^2$ needs to be estimated. We can define three-parameter relative displacement spectrum, $\mathrm{SDC}(T, \zeta, \tau)$, by

$$\mathrm{SDC}(T, \zeta, \tau) \equiv \max_{\forall t}\,[u^{\mathrm{r}}(t) + v(t)\tau - \tfrac{1}{2}a(t)\tau^2] \tag{21}$$

This spectrum can be computed on a routine basis during data processing and provided to the designer. Then, for a particular structure, the designer can evaluate τ for the end and other columns and read the maximum relative displacement from the corresponding response spectrum.

Response spectra for first-storey columns of multi-storey buildings

Modal analysis. Response of the ith mode of vibration of a MDOF system can be described by the differential equation[9]

$$\ddot{\xi}_i + 2\omega_i\zeta_i\dot{\xi} + \omega_i^2\xi_i = -\alpha_i\ddot{u}_0 \tag{22}$$

where ξ_i is the generalized co-ordinate, ω_i and ζ_i are the corresponding frequency and damping, and α_i is the mode participation factor. If $[\tilde{A}]$ is a $n \times n$ matrix whose columns contain the mode-shapes of the system, then the floor displacements in the horizontal direction (see Figure 3(a)) are

$$\underset{\sim}{d} = [\tilde{A}]\underset{\sim}{\xi} \tag{23}$$

and the displacement of the first floor is $d_1 = \tilde{A}_{11}\xi_1 + \tilde{A}_{12}\xi_2 + \cdots + \tilde{A}_{1n}\xi_n$. For $z(\omega)$ representing the Fourier transform of $\ddot{u}_0(t)$, and $\bar{z}(\omega_i)$ the mean value of $z(\omega)$, averaged over interval $\pi\zeta_i\omega_i$, we write[9]

$$\bar{d}_1^2 = \frac{\sqrt{2}}{T_{\mathrm{e}}}\left[\frac{\tilde{A}_{11}^2\alpha_1^2\bar{z}^2(\omega_1)}{4\zeta_1\omega_1^3} + \frac{\tilde{A}_{12}^2\alpha_2^2\bar{z}^2(\omega_2)}{4\zeta_2\omega_2^3} + \cdots + \frac{\tilde{A}_{1n}^2\alpha_n^2\bar{z}^2(\omega_n)}{4\zeta_n\omega_n^3}\right] \tag{24}$$

where $\bar{d}_1$ is the root mean square amplitude of the peaks of $d_1(t)$ and T_{e} is the equivalent duration of ground acceleration $\ddot{u}_0(t)$. The kth moment of the displacement transform squared for the first-storey response $d_1(t)$ is

$$m_{1k} = \frac{\pi}{4}\left[\frac{\tilde{A}_{11}^2\alpha_1^2\omega_1^k\bar{z}^2(\omega_2)}{\zeta_1\omega_1^3} + \frac{\tilde{A}_{12}^2\alpha_2^2\omega_2^k\bar{z}^2(\omega_2)}{\zeta_2\omega_2^3} + \cdots + \frac{\tilde{A}_{1n}^2\alpha_n^2\omega_n^k\bar{z}^2(\omega_n)}{\zeta_n\omega_n^3}\right] \tag{25}$$

Using m_{10}, m_{12} and m_{14}, we define the 'width' of the energy spectrum of response $d_1(t)$

$$\varepsilon_1^2 = \frac{m_{10}m_{14} - m_{12}^2}{m_{10}m_{14}} \tag{26}$$

The total number of peaks of $d_1(t)$ is

$$N_1 = \frac{T_e}{2\pi}\left(\frac{m_{14}}{m_{12}}\right)^{1/2} \tag{27}$$

The expected value of the peak response of the first floor, $d_1(t)_{\max}$, is[53,54]

$$E[d_1(t)_{\max}] \approx \bar{d}_1 \left\{ [\ln(1-\varepsilon_1^2)^{1/2} N_1]^{1/2} + \frac{\gamma}{2}[\ln(1-\varepsilon_1^2)^{1/2} N_1]^{-1/2} \right\} \tag{28}$$

where $\gamma = 0{\cdot}5772$. For design of first-storey columns, the maximum relative displacement of ith column is then approximately

$$\mathrm{SD}_i \approx \left\{ E^2[d_1(t)_{\max}] + (v_{\max}\tau_i)^2 + \left(\frac{1}{2}a_{\max}\tau_i^2\right)^2 \right\}^{1/2} \tag{29}$$

In the above equations (22)–(29), we neglected the effects of soil–structure interaction,[11,14] rotational components of strong motion,[12,15] contribution to response from other components of excitation and from modal interaction effects. All these contributions can be included, and the distribution functions for SD_i can be presented for a given n degree-of-freedom system. This requires some generalizations of the work on statistical response to earthquake excitation, and is outside the scope of this paper. Here we present only the basic ideas, trends and conditions for which the design of the first-storey columns must consider the differential motions of individual foundations.

First-mode approximation

For multi-storey buildings, which respond mainly in the first-mode of vibration, it is possible to define relative displacement spectra approximately, in terms of a parameter, δ, which is a function of the number of storeys and of the shape of the first mode of vibration. To explain δ, we consider the N-storey building in part (a) of Figure 3 and the equivalent SDOF oscillator in part (b) of the same figure. Both models are excited by horizontal ground acceleration $u_0(t)$ only. We neglect the effects of vertical ground acceleration, and of soil–structure interaction. All storey mass is lumped into the rigid floor slabs. The storey heights are h_1, $h_2, \ldots, h_N$. The resultant storey shears are $V_1, V_2, \ldots, V_n$. The storey displacements, relative to the moving ground are $d_i(t)$, $i = 1, 2, \ldots, N$.

The amplitude of the response, of a tall building, can be related to the response amplitude of the equivalent oscillator shown in part (b) of Figure 3. The equivalent oscillator has mass M_e, height H_e, damping constant C_e and natural period T_1, equal to the period of the fundamental mode of the multi-storey building. To determine the parameters of the equivalent oscillator, we first assume a mode shape for the first mode of vibration, $\phi_1(z)$, and assume that the mass is uniformly distributed along the building. Then, we represent the relative displacement of the top storey, $d_N(t)$, as

$$d_N(t) = A_1\phi_1(H)f(t) \tag{30}$$

and of the equivalent oscillator, $u_e(t)$, as

$$u_e(t) = A_e f(t) \tag{31}$$

In equations (30) and (31), $f(t)$ is a function of time that is factored out in both responses $d_N(t)$ and $u_e(t)$. Besides the requirement on the natural period, the equivalent oscillator must have height, mass and relative

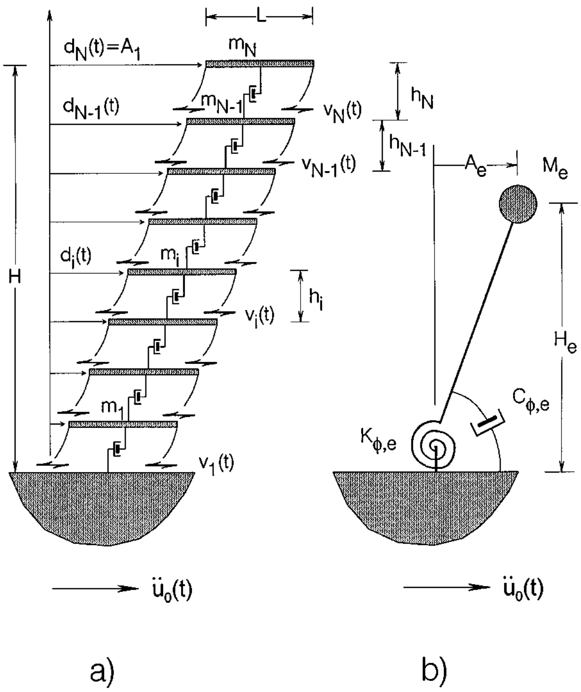

Figure 3. A N-storey building (a) and equivalent SDOF oscillator (b) with natural period equal to the fundamental period of the building. Both models are excited by synchronous motion of the base u_0

response amplitude such that the base shear, the overturning moment about the base and the kinetic energy of both structures are the same. These additional requirements imply

$$H_e = \left[\int_0^H z\phi_1(z)\,dz \right] \Big/ \left[\int_0^H \phi_1(z)\,dz \right] \tag{32}$$

$$A_e = A_1 \left[\int_0^H \phi_1^2(z)\,dz \right] \Big/ \left[\int_0^H \phi_1(z)\,dz \right] \tag{33}$$

and

$$M_e = \frac{M}{H} \left[\int_0^H \phi_1(z)\,dz \right]^2 \Big/ \left[\int_0^H \phi_1^2(z)\,dz \right] \tag{34}$$

where M is the total mass of the building. The stiffness and damping constant of the spiral spring and damper are such that the natural period of the equivalent oscillator is T_1 and the damping ratio ζ is equal to the modal damping ratio of the first mode of the multi-storey building.

Assuming that $\phi_1(z) = A_1 \sin(\pi z/2H)$, it follows that $H_e = 0{\cdot}64H$. Assuming that $\phi_1 = A_1 z/H$, $H_e = 0{\cdot}67H$. For actual buildings, m_i are different, and tend to decrease as i increases. This will reduce the factors 0·64 and 0·67, but we ignore this reduction here. We choose $A_1 = 1{\cdot}27$ for $\phi_1(z) \sim \sin(\pi z/2H)$, and $A_1 = 1{\cdot}50$ for $\phi_1(z) \sim z/H$.

Let $\mathrm{SD}(T_1, \zeta)$ represent the peak of the relative displacement response of the equivalent oscillator. Then the maximum relative displacement of the first storey of the N-storey building in Figure 3(a), associated with the first-mode response, is

$$|d_1|_{max} = \delta\, \mathrm{SD}(T_1, \zeta) \tag{35}$$

The factor δ has value 1 if $N = 1$ and if $N > 1$

$$\delta = \begin{cases} 1{\cdot}27 \sin(\pi h_1/2H) \sim 1{\cdot}27 \sin(\pi/2N) & \text{(sinusoidal mode shape)} \\ \dfrac{h_1}{H} \sim 1{\cdot}5/N & \text{(straight line mode shape)} \end{cases} \tag{36}$$

The expression for δ can be simplified further. For example, if we assume that $T_1 \approx 0{\cdot}1\, N$, where N is the number of stories, and if we take the straight line approximation for the mode shape, δ can be expressed only in terms of the fundamental period of the building

$$\delta \approx \begin{cases} 1{\cdot}5/(10\,T_1); & T_1 > 0{\cdot}15 \\ 1; & T_1 < 0{\cdot}15 \end{cases} \tag{37}$$

By equations (36) and (37), we illustrated two simple functional forms for δ versus H or N. The actual mode shape will alter δ in equation (36), but not enough to affect the subsequent results significantly.

Next, we consider the model in Figure 3 of a multi-storey building, excited by differential motion of the first-storey columns $u_i^{\mathrm{r}}(t) + u_0(t)$. The relative displacement response at the first floor is $d_1(t) \approx \delta u_{\mathrm{e}}(t)$ (Figure 4).

We define a more general relative response spectrum SDC(T, δ, ζ, τ), than the one in equation (21), which depends on an additional parameter, δ,

$$\mathrm{SDC}(T, \delta, \zeta, \tau) \equiv \max_{\forall t} \left[u^{\mathrm{r}}(t)\delta + v(t)\tau - \tfrac{1}{2}a(t)\tau^2\right] \tag{38}$$

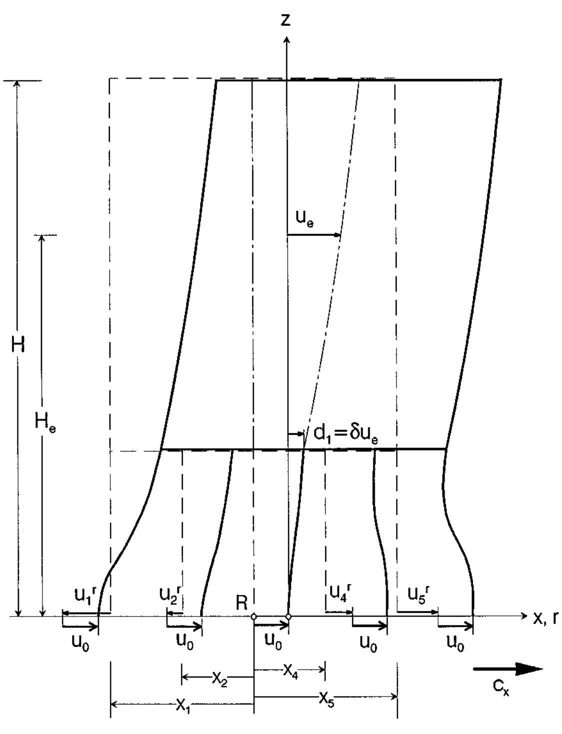

Figure 4. A multi-storey building excited by asynchronous motion at the base of the first storey columns. Point R and the z-axis move with displacement u_0 that satisfies the condition $\sum_1^n k_i u_i = u_0 \sum_1^n k_i$, where u_i is the absolute displacement of the ith column. u_{e} is the relative displacement of the equivalent SDOF oscillator for this building excited by acceleration $\ddot{u}_0$. d_1 is the relative displacement of the first storey

The case $\delta = 1$ corresponds to a one-storey structure. For multi-storey buildings, T refers to the fundamental period, T_1.

In equation (38), $u^r(t)$ is the response of the equivalent SDOF oscillator for the multi-storey building to motion $u_0(t)$, and it can be calculated by the means of the Duhamel's integral.[4] An approximation for the SDC-spectrum defined by equation (38) is

$$\mathrm{SDC}(T, \delta, \zeta, \tau) \approx [\delta^2\, \mathrm{SD}^2(T, \zeta) + (v_{\max}\tau)^2 + (\tfrac{1}{2}a_{\max}\tau^2)^2]^{1/2} \tag{39}$$

where $\mathrm{SD}(T, \zeta)$ is the classical relative spectral displacement and $v_{\max}$ and $a_{\max}$ are the peak velocity and acceleration of the motion of reference point R. In the next section, we compare results for SDC-spectrum calculated via equation (38) and approximated by the expression in equation (39).

RESULTS AND ANALYSIS

The relative response $u^r(t)$ increases with increasing period of the SDOF system, $T = 2\pi/\omega = 2\pi\sqrt{(m/k)}$, and as $T \to \infty$, $u^r(t) \to -u_0(t)$. The relative displacement spectrum $\mathrm{SD}(T, \zeta) = \max_{\forall t}|u^r(t)|$ thus increases from zero to $|u_0(t)|_{\max}$ as T increases from zero to infinity. This behaviour can be seen from the plot of $\mathrm{SD}(T, \zeta)$ in Figures 5 and 6. These figures also show the spectra $\mathrm{SDC}(T, \delta, \zeta, \tau)$ for the S16W component of strong motion recorded at station #53 of the Los Angeles Strong Motion Network, during the Northridge, CA, earthquake of 17 January 1994. The response $u^r(t)$ was obtained from instrument, baseline, misalignment and cross-axis sensitivity[55] corrected acceleration time history $a(t)$. Figure 5 corresponds to $\zeta = 0$ and Figure 6 to $\zeta = 0{\cdot}05$, and in both figures $\delta = 1$. Both figures show spectra for τ between 0·001 and 0·1 (where for the ith column, at distance x_i from the reference point R, $\tau = Ax_i/\beta_{\mathrm{av}}$). The solid lines correspond to SDC-spectra

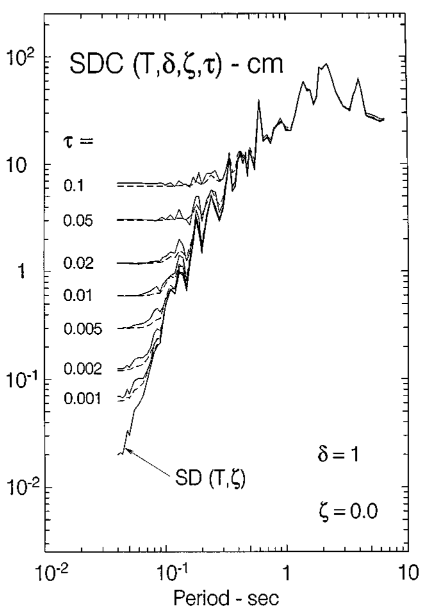

Figure 5. The newly defined spectra $\mathrm{SDC}(T, \delta, \zeta, \tau_i)$ for the S16W component of the accelerogram recorded at station #53 of the Los Angeles Storey Motion Network during the Northridge, CA, earthquake of 17 January 1994 ($M = 6{\cdot}7$), at epicentral distance 6 km. All spectra correspond to damping ratio $\zeta = 0$ and to $\delta = 1$ (one-storey building). Different spectra correspond to different values of parameter $\tau = Ax/\beta_{\mathrm{av}}$ ranging from 0·001 to 0·1. x is the distance of the column from point R in the undeformed configuration, and β_{av} is the average shear wave velocity in the top 30 m of soil. The solid lines correspond to SDC-spectra calculated exactly, and the dashed lines to the approximate estimate via relative spectral displacement $\mathrm{SD}(T, \zeta)$, also shown in the figure, and the peak ground velocity and acceleration

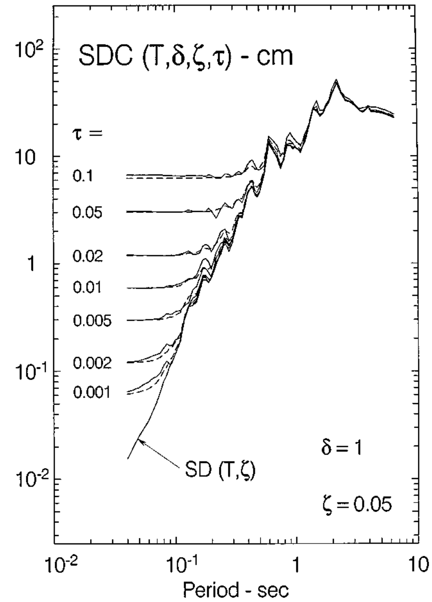

Figure 6. Same as Figure 5 but for damping ratio $\zeta = 0{\cdot}05$

calculated from equation (38), and the dashed lines show the estimate by the approximation in equation (39). For the S16W component of strong motion at station USC #53, peak amplitudes of strong motion were $u_{0,\max} = 12{\cdot}4$ cm, $v_{\max} = 59{\cdot}8$ cm/s and $a_{\max} = 381$ cm/s^2 (4·88 in, 23·5 in/s and 150 in/s^2, respectively).

Figures 5 and 6 show that for some period T_* motions for $T < T_*$ lead to approximately constant $\mathrm{SDC}(T, \delta, \zeta, \tau)$. For these periods, the peak of relative displacement for column design is dominated by $[v(t)\tau - \frac{1}{2}a(t)\tau^2]_{\max}$ and the peak shear forces result from pseudo-static deformation caused by large differential motions. For $T > T_*$, the contribution of the term $v(t)\tau - \frac{1}{2}a(t)\tau^2$ to the relative motion of columns becomes negligible and the peak shear forces are governed by the relative dynamic response $d_1(t) = \delta u^{\mathrm{r}}(t)$.

Figure 7 illustrates the amplification factor $\mathrm{SDC}(T, \delta, \zeta, \tau)/\delta\, \mathrm{SD}(T, \zeta)$ for shear forces at the first floor of structures for $\tau = 0{\cdot}001$, 0·02, 0·005, 0·01, 0·02, 0·05 and 0·1 and for $\delta = 1$. It is seen that when $T = 0{\cdot}1$ s, for example, this factor is in the range from about 1 (for $\tau = 0{\cdot}001$) to about 50 (for $\tau = 0{\cdot}1$). A one-storey structure, with natural period $T \approx 0{\cdot}1$ s, damping $\zeta = 0{\cdot}05$, at a site with $\beta_1 = 300$ m/s, and with plan dimensions equal to 30 m, will have $\tau_{\max} \approx (1 * 15)/300 = 0{\cdot}05$ and the amplification factor SDC (0·1, 1·0, 0·05, 0·05)/ SD(0·1, 0·05) ≈ 20.

Figures 8 and 9 show, respectively, SDC-spectra and the ratio $\mathrm{SD}(T, \delta, \zeta, \tau)/\delta\, \mathrm{SD}(T, \zeta)$ for a multi-storey building, for damping ratio $\zeta = 0{\cdot}05$ and response associated with the fundamental mode only. These spectra depend on parameter δ which we chose to relate to the fundamental period T_1 by $\delta = 1{\cdot}5/(10\,T_1)$ (see equation (37)). This relationship for $T_1 > 0{\cdot}15$, results in progressively more important role of δ for increasing period (Figure 8). From Figure 9, it is seen that the amplification factor $\mathrm{SDC}(T, \delta, \zeta, \tau)/\delta\, \mathrm{SD}(T, \zeta)$ is now larger for $T = T_1 > 0{\cdot}15$ relative to the case for $\delta = 1$ (Figure 7). It experiences minimum amplitudes near the peak of $\delta\, \mathrm{SD}(T, \zeta)$ and then grows again for longer T_1. A ten-storey structure, with natural period approximately equal to 1 s and fraction of critical damping $\zeta = 0{\cdot}05$, and with plan dimensions say ~ 30 m (100 ft), will have $\tau \cong (1{\cdot}0)(30/2)/300 = 0{\cdot}05$, assuming $\beta_{\mathrm{av}} = 300$ m/s. Figure 9 indicates that the peak shear force in the first-storey end columns will be double relative to the results ignoring wave propagation and strain deformations in the soil.

Figure 9 suggests that the analyses of base-isolated structures, for which the fundamental period is increased by 'soft' isolation devices, must consider this contribution from differential motions in the

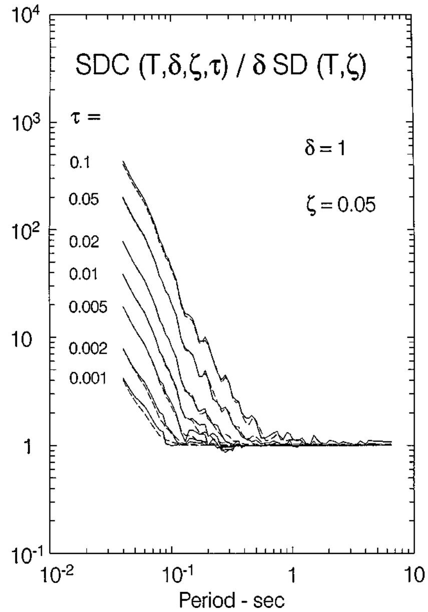

Figure 7. Ratio of the new relative displacement spectra for columns and the old relative displacement spectra, $SDC(T, \delta, \zeta, \tau)/\delta SD(T, \zeta)$, both shown in Figure 6

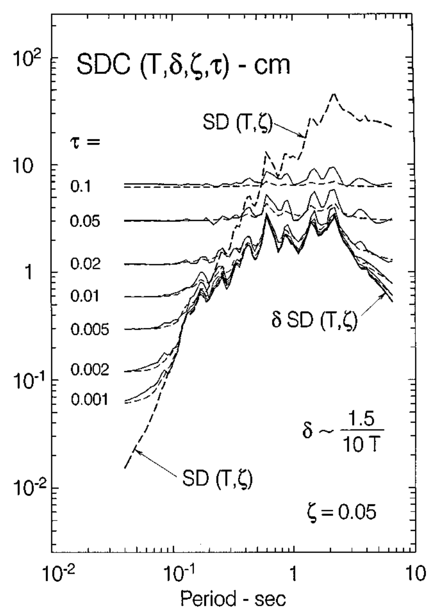

Figure 8. Same as Figure 5 but for damping ratio $\zeta = 0{\cdot}05$ and for multi-storey buildings. The parameter δ is a function of the period, $\delta = 1{\cdot}5/(10\,T)$ as per equation (29)

foundation soil, when the isolation devices are supported by individual foundations. The natural period of base-isolated structures is longer relative to the corresponding fixed-base period of the same structure. One expected benefit of this shift in natural period is in the hypothesized decrease of acceleration spectrum amplitudes for $T > T_p$ (T_p is the period where the acceleration spectrum is the largest). This hypothesis is

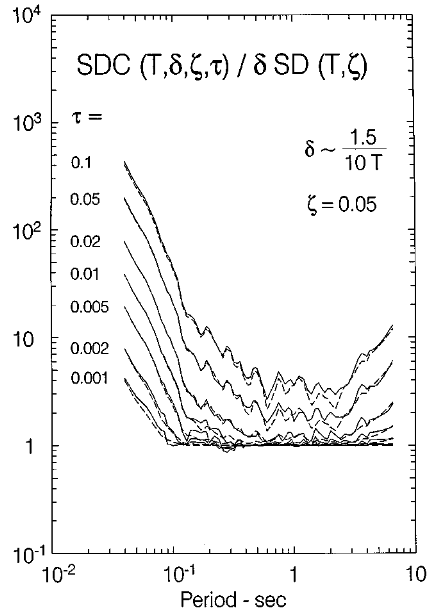

Figure 9. Ratio of the new relative displacement spectra for columns and the old relative displacement spectra, $\mathrm{SDC}(T, \delta, \zeta, \tau_i)/\delta\,\mathrm{SD}(T, \zeta)$, both shown in Figure 8

valid only for far-field strong ground motion. In the near field, the acceleration spectrum, especially for large earthquakes, will have 'flat' amplitudes in a broad long-period range. These amplitudes may begin to fall of only for very long periods, much longer than the fundamental period of the base-isolated building.[56,57] The analysis in this paper shows that the contributions from differential motions of separate footings will contribute further relative displacements, which will increase with increasing natural period T, when $T > T_p$.

SUMMARY AND CONCLUSIONS

We showed that the linear response of simple structures supported by individual columns, which experience differential motions at their foundations, can be described by response spectra, defined for relative motion with respect to a point R, whose displacement, $u_0(t)$, is a weighted average of the motions at the base of the columns (see equation (5)). Then, essentially all published results on the response spectrum method remain valid, provided this reference point is used in the analyses. The peak relative displacement of columns which are very close to the reference point R ($x_i \sim 0$) can be calculated via the classical two-parameter relative displacement spectrum, $\mathrm{SD}(T, \zeta)$. For the first-storey columns that are at distance x_i from the reference point, the four-parameter relative displacement spectra, $\mathrm{SDC}(T, \delta, \zeta, \tau)$, should be used. The two additional parameters are the factor δ, representing the ratio of the peak relative response of the first floor to $\mathrm{SD}(T, \zeta)$ and the parameter $\tau = Ax_i/\beta_{av}$, which is a measure of the time required for a wave to propagate from reference point R (see Figure 2) to the ith column (distance x_i) with velocity of the shear waves in the soil beneath the structure, β_{av}.

The popularity of the concept of response spectrum in earthquake resistant design is due to its simplicity. All structures are characterized only by two parameters, the natural period, T, and the fraction of critical damping, ζ, and its amplitudes are independent of the geometry or the material properties of the structure. The spectrum $\mathrm{SDC}(T, \delta, \zeta, \tau)$ retains this important property (as the additional parameters δ and τ are also simple), but also takes into consideration the spatial variation of ground motion. Therefore, it is a useful tool for design, to estimate peak shear forces and peak bending moments of first-storey columns of structures.

The amplitudes of the spectrum $\mathrm{SDC}(T, \delta, \zeta, \tau)$ can be computed directly by evaluating the relative response, $u^{\mathrm{r}}(t)$, via the Duhamel's integral,[58–60], multiplying it by δ and then adding the contribution from strain, expressed in terms of the ground velocity, $v(t)$, and the ground acceleration, $a(t)$ (see equation (36)). Alternatively, $\mathrm{SDC}(T, \delta, \zeta, \tau)$ can be computed from empirical scaling equations[62–64] for the classical relative spectral displacement, $\mathrm{SD}(T, \zeta)$, and for the peak ground velocity and acceleration, $v_{\max}$ and $a_{\max}$,[65,66] via equation (39). The examples presented in this paper show that the expression in equation (39) leads to results that approximate those by equation (38). For use in design, spectra $\mathrm{SDC}(T, \delta, \zeta, \tau)$ can be estimated for a scenario earthquake or for a family of all possible earthquake ground motions during the life of a structure, in the framework of probabilistic seismic hazard analysis.[67–70] The outcome of the latter approach will be uniform probability SDC-spectra and the associated microzonation maps.[67,70] A collection of such maps, for different combinations of values of spectral period, T, damping ratio, ζ, and the newly defined parameters δ and τ, can be prepared for direct use in design of columns.

SDC-spectra have been illustrated in this paper for a horizontal component of a recording in the near field of the Northridge, CA, earthquake of 17 January 1994. The results indicate that the increase in the shear forces for peripheral columns (on individual foundations), during this earthquake, caused by differential ground motion was significant, so that one must consider this effect in design of new and in retrofitting of existing structures. In particular, the results lead to the conclusion that for high frequency (stiff) structures, with moderate and large horizontal dimensions, the shear forces and the associated bending moments in the peripheral columns will exceed the estimates based on the original relative displacement spectra $\mathrm{SD}(T, \zeta)$, by factors which can be large. As noted by Zembaty and Krenk[40,41] and confirmed by this study, this is at variance with results of some previous studies, based on random vibration theory, which do not consider u_i^{r} explicitly. The main difference between the approach in this paper and the studies which use random vibration theory is in the representation of the differential motions. The latter studies use cross-correlation functions to describe differences in motion of individual supports, while the study in this paper uses more direct physical representation of the differential motions.

In this paper, we presented $\mathrm{SDC}(T, \delta, \zeta, \tau)$ with example emphasizing the use of response spectra in buildings. Mutatis mutandis, with $\delta = 1$, these results and our findings apply to the anlyses of bridges and particularly to the portions of long bridges where the deck is continuously supported by two or more columns. For simplicity in analysis of multi-storey structures, we illustrated the relative motion of the first storey in terms of the parameter δ, considering the first mode of response only. Using the results and formulation of Gupta and Trifunac,[11–14] the parameter δ can be generalized to include contribution of all modes of the response.

The above analysis considered only the simple consequences of differential motion of foundations on separate footings. We analysed the effects of radial strains and the response of structures which are oriented to coincide with the plane containing the earthquake source, propagation path and the site of the structure. Obviously, other components of strain[44,51] and of ground distortion and warping[52] will contribute to the overall response and to the moments and shears in the first-storey columns. Detailed analyses of these contributions to the response is beyond the scope of this paper.

It is concluded that (1) the concept of response spectrum can be generalized to include contributions to shears and moments in first-storey columns from differential ground motions, and (2) SDC spectrum should be further refined and used in design. The classical response spectrum may not provide sufficient seismic protection, particularly for high frequency (stiff) structures, with moderate and large horizontal dimensions, supported by individual column foundations, on softer soils.

Equation (5) in this paper represents an averaging filter, and the degree to which it filters the incident motions is related to the separation distance between the end columns (L in Figure 2). Excitation of our structural model by synchronous motion $u_0(t)$, along with quasi static forces in the columns, does lead to frequency intervals where the overall response is reduced significantly. This occurs only for very large L (e.g. $L = |x_n - x_1| > 200$ m) or for exceptionally small β_{av}, which may be of little practical use.

Over 'short' separation distances (e.g. $L < 50$–100 m), the strong earthquake displacement is more coherent and 'deterministic' than one is lead to believe after perusing various published studies of the coherence of strong motion accelerations.[19–24,26–28,37–41,46,47] Ground displacements result from $1/\omega^2$

filtering of strong motion acceleration, and thus derive their nature mostly from long wavelengths. Since the contribution to shear forces in the first-storey columns from the quasi static component of motion also depends on the amplitudes of differential ground displacements, for small separation distances, the first order (one term) Taylor series approximation works well because of this coherence of ground displacements.

The first-order (one term) Taylor series approximation

$$u_i^{\mathrm{r}}(t) \approx -v(t)\tau_i \tag{40}$$

is equivalent to assuming constant strain field over the distance L (see Figure 2), and for this case our reference point R may be thought of as being fixed to the ground surface and moving with displacement $u_0(t)$. Equation (5) however is general and does not require R to be a 'fixed point'. For large L (i.e. large x_1 and x_n in Figure 2) and for wavelengths λ comparable to and smaller than $\sim L/4$, equation (40) ceases to hold and other representations for $u_i^{\mathrm{r}}(t)$ must be used. But for typical wave velocities in soils and in sediments in the Southern California region, $\tau \lesssim 0{\cdot}1$ will suffice for many and even for some 'large' structures, and for the constant strain field approximation.

Filtering (averaging) of ground motion, which leads to reduction of the foundation displacements, may be more a popular myth created by numerous stochastic simulations of responses of single, large, and absolutely rigid foundations, but with little if any support from actually recorded motions in building foundations.[71,72] Reduction of the relative response $u^{\mathrm{r}}(t)$ of long structures, with columns on multiple separate foundations, is more plausible, but again may be exaggerated by examples which involve unrealistically large separation of columns (often hundreds of metres).[40,41] The simple models and the assumptions in this paper do not contradict the results of previous studies. We merely consider realistic separation distances (less than 40 to 50 m for buildings, and realistic shear wave velocities in the soil (e.g. $100 \lesssim \beta_{\mathrm{av}} \lesssim 1000$ m/s) for which these reductions are small.

REFERENCES

1. H. Benioff, 'The physical evaluation of seismic destructiveness', *Bull. seism. soc. Am.* **24**, 389–403 (1934).
2. M. A. Biot, 'A mechanical analyzer for the prediction of earthquake stresses', *Bull. seism. soc. Am.* **31**, 151–171 (1941).
3. R. L. Wiegel, Earthquake Engineering, Chapter 4, Prentice-Hall, Englewood Cliffs, New Jersey, 1970, pp. 54–63.
4. M. D. Trifunac, 'Strong-motion accelerograms, III, response spectra' (with Introduction by D. E. Hudson and Commentary by A. G. Brady), *Earthquake Eng. Res. Lab., Report EERL 72-80*, Earthquake Eng. Res. Lab., Calif. Inst. of Technol. Pasadena, CA, 1972.
5. M. D. Trifunac, 'Preliminary empirical model for scaling Fourier amplitude spectra of strong ground acceleration in terms of earthquake magnitudes, source to station distance and recording site conditions', *Bull. seism. soc. Am.* **66**, 1343–1373 (1976).
6. M. D. Trifunac, 'Response spectra of earthquake ground motion', *ASCE*, **104**(5), 1081–1097 (1978).
7. M. D. Trifunac and J. G. Anderson, 'Preliminary empirical model for scaling absolute acceleration spectra', *Report No. CE 77-03*, Dept. of Civil Eng., Univ. of Southern California, Los Angeles, CA, 1977.
8. M. A. Biot, 'Analytical and experimental methods in engineering seismology', *Trans. ASCE*, **108**, Paper No. 2183, p. 365 (1943).
9. A. Amini and M. D. Trifunac, 'Statistical extension of response spectrum superposition', *Int. j. soil dyn. earthquake eng.* **4**(2), 54–63 (1985).
10. I. D. Gupta and M. D. Trifunac, 'Order statistics of peaks in earthquake response', *J. eng. mech. div. ASCE* **114**(10), 1605–1627 (1988).
11. I. D. Gupta and M. D. Trifunac, 'Probabilistic spectrum superposition for response analysis including the effects of soil–structure interaction', *J. prob. eng. mech.* **5**(1), 9–18 (1990).
12. V. K. Gupta and M. D. Trifunac, 'Response of multistoried buildings to ground translation and rocking during earthquakes', *J. prob. eng. mech.* **5**(3), 138–145 (1990)
13. V. K. Gupta and M. D. Trifunac, 'Response of multistoried buildings to ground translation and torsion during earthquakes', *European earthquake eng.*, **IV**(1), 34–42 (1990).
14. V. K. Gupta and M. D. Trifunac, 'Seismic response of multistoried buildings including the effects of soil structure interaction', *Soil dyn. earthquake eng.* **10**(8), 414–422 (1991).
15. V. K. Gupta and M.D. Trifunac, 'Effects of ground rocking on dynamic response of multistoried buidlings during earthquakes', *Struct. eng./earthquake eng.*, JSCE **8**(2), 43–50 (1991).
16. M. I. Todorovska, 'Order statistics of functionals of strong ground motion', *Soil dyn. earthquake eng.* **13**(6), 399–405 (1994).
17. M. I. Todorovska, 'A note on the distribution of amplitudes of peaks in structural response including uncertainties of the exciting ground motion and the structural model', *Soil dyn. earthquake eng.* **14**(3), 211–217 (1995).
18. J. L. Bogdanoff, J. E. Goldberg and A. J. Schiff, 'The effect of ground transmission time on the response of long structures', *Bull. seism. soc. Am.* **55**, 627–640 (1965).
19. C. H. Loh, J. Penzien and Y. B. Tsai, 'Engineering analysis of SMART-1 array accelerograms', *Earthquake eng. struct. dyn.* **10**, 575–591 (1982).
20. R. S. Harichandran and E. H. Vanmarcke, 'Stochastic variation of earthquake ground motion in space and time', *J. eng. mech. div. ASCE* **112**(2), 154–174 (1986).

21. H. Hao, 'Effects of spatial variations of ground motion on large multiply-supported structures', Univ. of California at Berkeley, *Report No. EERC 89-06*, Earthquake Eng. Res. Lab., Berkeley, CA, 1989.
22. R. S. Harichandran and W. Wang, 'Response of simple beam to spatially varying earth-quake excitation', *J. eng. mech. div. ASCE* **114**, 1526–1541 (1988).
23. R. S. Harichandran and W. Wang, 'Response of indeterminate two-span beam to spatially varying seismic excitation', *Earthquake eng. struct. dyn.* **19**, 173–187 (1990).
24. A. Zerva, 'Effect of spatial variability and propagation of seismic ground motions on the response of multiply supported structures', *Prob. eng. mech.* **6**, 212–221 (1991).
25. I. Kashefi and M. D. Trifunac, 'Investigation of earthquake response of simple bridge structures', *Dept. of Civil Eng.*, *Report No. CE 86-02*, Univ. of Southern California, Los Angeles, CA, 1986.
26. F. Perotti, 'Structural response to non-stationary multiple support random excitation', *Earthquake eng. struct. dyn.* **19**, 513–527 (1990).
27. C. -H. Hyun, C. B. Yun and D. G. Lee, 'Nonstationary response analysis of suspension bridges for multiple support excitations', *Prob. eng. mech.* **7**(1), 27–35 (1992).
28. H. Hao, 'Response of multiply supported rigid plate to spatially correlated seismic excitation', *Earthquake eng. struct. dyn.* **20**, 821–838 (1991).
29. M. I. Todorovska and V. W. Lee, 'Seismic waves in buildings with shear walls or central core', *J. eng. mech. div. ASCE* **115**(12), 2669–2686 (1989).
30. M. I. Todorovska and M. D. Trifunac, 'Antiplane earthquake waves in long structures', *J. eng. mech. div. ASCE* **115**(12), 2687–2708 (1989).
31. M. I. Todorovska and M. D. Trifunac, 'A note on the propagation of earthquake waves in buildings with soft first floor', *J. eng. mech. div. ASCE* **116**(4), 892–900 (1990).
32. M. I. Todorovska and M. D. Trifunac, 'A note on excitation of long structures by ground waves', *J. eng. mech. div. ASCE* **116**(4), 952–964 (1990).
33. S. Kojić and M. D. Trifunac, 'Earthquake response of arch dams to nonuniform canyon motion', *Dept. of Civil Eng.*, *Report No. CE 88-03*, Univ. Southern California, Los Angeles, CA, 1988.
34. S. Kojić and M. D. Trifunac, 'Earthquake stresses in arch dams: I—theory and antiplane excitation', *J. eng. mech. div. ASCE* **117**(3), 532–552 (1991).
35. S. Kojić and M. D. Trfunac. 'Earthquake stresses in arch dams: II excitation by SV, P and Rayleigh waves', *J. eng. mech. div. ASCE* **117**(3), 553–574 (1991).
36. M. Berrah and E. Kausel, 'Modified response spectrum model for the design of structures subjected to spatially varying seismic excitations', *MIT Research Report R90-2*, Massachusetts Institute of Technology, Cambridge, MA, 1990.
37. R. Betti and G. F. Panariello, 'Active control of structures subjected to spatially varying earthquake excitation', *Proc. 1st world conf. on struct. control*, vol. **2**, TP2-79-TP2-88, 1994.
38. A. Der-Kiureghian and A. Neuenhofer, 'Response spectrum method for multisupport seismic excitation', *Earthquake eng. struct. dyn.* **21**, 713–740 (1992).
39. T. Okubo, T. Arakawa and K. Kawashima, 'Preliminary analysis of finite ground strains induced during earthquake and effect of spatial ground motions on structural response', *Int. symp. on lifeline earthquake eng. 4th U.S. National Conf. on Pressure Vessels and Piping Technology*, ASME, Portland Oregon, U.S.A., 1983.
40. Z. Zembaty and S. Krenk, 'Spatial seismic excitations and response spectra', *J. eng. mech. div. ASCE* **119**, 2449–2459 (1993).
41. Z. Zembaty and S. Krenk, 'Response spectra of spatial seismic ground motion', *10th European conf. earthquake eng.* vol. **2**, Vienna, Austria, 1994, pp. 1271–1275.
42. V. W. Lee and M. D. Trifunac, 'Torsional accelerograms', *Int. j. soil dyn. earthquake eng.* **4**(3), 132–139 (1985).
43. V. W. Lee and M. D. Trifunac, 'Rocking strong earthquake acceleration', *Int. j. soil. dyn. earthquake eng.* **6**(2), 75–89 (1987).
44. M. D. Trifunac and V. W. Lee, 'Peak surface strains during strong earthquake motion', *Soil dyn. earthquake eng.* **15**(5), 311–320 (1996).
45. M. D. Trifunac, M. I. Todorovska and S. S. Ivanović, 'Peak velocities and peak surface strains during Northridge, California', earthquake of 17 January 1994, *Soil dyn. earthquake eng.* **15**(5), 301–310 (1996).
46. M. J. O'Rourke and G. Castro, 'Effects of seismic wave propagation upon buried pipelines', *Earthquake eng. struct. dyn.* **8**, 455–467 (1980).
47. M. J. O'Rourke, G. Castro and I. Hossian, 'Horizontal soil strain due to seismic waves', *J. geotech. eng. div. ASCE* **110**, 1173–1187 (1984).
48. M. D. Trifunac, 'Response envelope spectrum and interpretation of strong earthquake ground motion', *Bull. seism. soc. Am.* **61**, 343–356 (1971).
49. G. N. Bycroft, 'Differential ground motion array at Hollister municipal airport, California', *Open File Report 83–327*, U.S. Geological Survey, 1983.
50. K. Moslem and M. D. Trifunac, 'Spectral amplitudes of strong earthquake accelerations recorded in buildings', *Soil dyn. earthquake eng.* **6**(2), 100–107 (1987).
51. V. W. Lee, 'Surface strains associated with strong earthquake shaking', *Proc. JSCE*, **422**(I-14), 187–194 (1990).
52. M. D. Trifunac, 'Curvograms of strong ground motion', *J. eng. mech. div. ASCE* **116**(6), 1426–1432 (1990).
53. I. D. Gupta and M. D. Trifunac, 'Investigation of nonstationarity in stochastic seismic response of structures', *Report No. CE 96-01*, Dept. of Civil Eng., Univ. of Southern California, Los Angeles, CA.
54. F. E. Udwadia and M. D. Trifunac, 'Characterization of response spectra through the statistics of oscillator response', *Bull. seism. soc. Am.* **64**, 205–219 (1974).
55. M. I. Todorovska, E. I. Novikova, M. D. Trifunac and S. S. Ivanović, 'Correction for misalignment and cross-axis sensitivity of strong earthquake motion recorded by SMA-1 acceleraographs', *Report No. CE 95-06*, Dept. of Civil Eng., Univ. of Southern California, Los Angeles, CA, 1995.

56. M. D. Trifunac, 'Long period Fourier amplitude spectra of strong motion acceleration', *Soil. dyn. earthquake eng.* **12**(6), 363–382 (1993).
57. M. D. Trifunac, 'Pseudo relative velocity spectra of earthquake ground motion at long periods', *Soil dyn. earthquake eng.* **14**(5), 331–346 (1995).
58. M. D. Trifunac and V. W. Lee, 'Routine computer processing of strong motion accelerograms', *Report EERL 73-03*, Earthquake Eng. Res. Lab., Calif. Inst. of Technol. Pasadena, CA, 1973.
59. M. D. Trifunac and V. W. Lee, 'Automatic digitization and processing of strong motion accelerograms', Parts I and II, *Report No. CE 79-15*, Dept. of Civil Eng., Univ. of Southern Calfornia, Los Angeles, CA, 1979.
60. V. W. Lee and M. D. Trifunac, 'Automatic digitization and processing of accelerograms using PC', *Dept. of Civil Eng., Rep. No. CE 90-03*, Univ. of Southern California, Los Angeles, CA, 1990.
61. V. W. Lee, 'Empirical scaling of pseudo relative velocity spectra of recorded strong earthquake motion in terms of magnitude, and both local soil and geologic site classifications', *Earthquake eng. eng. vibration* **9**(3), 9–29 (1989).
62. V. W. Lee, 'Scaling PSV spectra in terms of site intensity, and both local soil and geological site classifications', *European earthquake eng.* **IV**(1), 3–12 (1990).
63. V. W. Lee, 'Correlation of pseudo relative velocity spectra with site intensity, local soil classification and depth of sediments', *Soil dyn. earthquake eng.* **10**(3), 141–151 (1991).
64. V. W. Lee, 'Scaling PSV spectra from earthquake magnitude, local soil and geological depth of sediments', *J. geotech. eng. div. ASCE* **119**(1), 108–126 (1993).
65. M. D. Trifunac, 'Preliminary analysis of the peaks of strong earthquake ground motion—dependence of peaks on earthquake magnitude, epicentral distance and the recording site conditions', *Bull. seism. soc. Am.* **66**, 189–219 (1976).
66. V. W. Lee, M. D. Trifunac, M.I. Todorovska and E. I. Novikova, 'Empirical equations describing attenuation of peaks of strong ground motion in terms of magnitude, distance, path effects and site conditions', *Report No. CE 95-02*, Dept. of Civil Eng., Univ. Southern California, Los Angeles, CA, 1995.
67. M. D. Trifunac, 'Seismic microzonation mapping via uniform risk spectra', *Proc. 9th world conf. earthquake eng.*, vol. VII, Tokyo-Kyoto, Japan, 1988, pp. 75–80.
68. M. D. Trifunac, 'A microzonation method based on uniform risk spectra', *Int. j. soil. dyn. earthquake eng.* **9**(1), 34–43 (1990).
69. M. I. Todorovska, I. D. Gupta, V. K. Gupta, V. W. Lee and M. D. Trifunac, 'Selected topics in probabilistic seismic hazard analysis', *Report No. CE 95-08*, Dept. of Civil Eng., Univ. of Southern California, Los Angeles, CA, 1995.
70. M. I. Todorovska and M. D. Trifunac, 'Hazard mapping of normalized peak strain in soil during earthquakes—microzonation of a metropolitan area', *Soil dyn. earthquake eng.* **15**(5), 321–329 (1996).
71. V. W. Lee, M. D. Trifunac and E. C. Feng, 'Effects of foundation size on Fourier spectrum amplitudes of earthquake accelerations recorded in buildings', *Soil dyn. earthquake eng.* **1**(2), 52–58 (1982).
72. K. Moslem and M. D. Trifunac, 'Spectral amplitudes of strong earthquake accelerations recorded in buildings', *Soil dyn. earthquake eng.* **6**(2) 100–107 (1987).